Journal of Medicinal Chemistry

Article

Selective inhibitors of human liver carboxylesterase based upon a #-lapachone scaffold: Novel reagents for reaction profiling

M. Jason Hatfield, Jingwen Chen, Ellie M Fratt, Liying Chi, John C. Bollinger, Randall J Binder, John Bowling, Janice L. Hyatt, Jerrod Scarborough, Cynthia Jeffries, and Philip M Potter

J. Med. Chem., **Just Accepted Manuscript** • DOI: 10.1021/acs.jmedchem.6b01849 • Publication Date (Web): 23 Jan 2017

Selective inhibitors of human liver carboxylesterase based upon a β-lapachone scaffold: Novel reagents for reaction profiling

M. Jason Hatfield[†,1], Jingwen Chen[†,1], Ellie M. Fratt[1], Liying Chi[1], John C. Bollinger[2], Randall J. Binder[1], John Bowling[1], Janice L. Hyatt[1], Jerrod Scarborough[1], Cynthia Jeffries[1], Philip M. Potter[*,1]

1 - Department of Chemical Biology and Therapeutics,

2 - Department of Structural Biology,

St. Jude Children's Research Hospital, Memphis, TN 38105, United States

[†] – These authors contributed equally to this work.

[*] Corresponding author.

Philip M. Potter

Department of Chemical Biology and Therapeutics,

St. Jude Children's Research Hospital,

262 Danny Thomas Place,

Memphis,

TN 38105, United States

Tel: 901-595-6045

Fax: 901-595-4293

E-mail: phil.potter@stjude.org.

ABSTRACT

Carboxylesterases (CE) are ubiquitous enzymes that are responsible for the metabolism of xenobiotics, including drugs such as irinotecan and oseltamivir. Inhibition of CEs significantly modulates the efficacy of such agents. We report here that β-lapachone is a potent, reversible CE inhibitor with K_i values in the nanomolar range. A series of amino and phenoxy analogues have been synthesized and while the former are very poor inhibitors, the latter compounds are highly effective in modulating CE activity. Our data demonstrate that tautomerism of the amino derivatives to the imino forms likely accounts for their loss in biological activity. A series of N-methylated amino derivatives, which are unable to undergo such tautomerism, were equal in potency to the phenoxy analogues, and demonstrated selectivity for the liver enzyme hCE1. These specific inhibitors, which are active in cell culture models, will be exceptionally useful reagents for reaction profiling of esterified drugs in complex biological samples.

INTRODUCTION

Carboxylesterases (CE) are members of the esterase class of enzymes that hydrolyze esters into their corresponding carboxylic acids and alcohols.[1] These enzymes are present in essentially all organisms and are thought to play a protective role against xenobiotics that may contain these chemotypes.[2] As such, numerous biologically important small molecules contain ester groups including xenobiotics (e.g., cocaine and heroin[3]) as well as many clinically used agents (for example, irinotecan (CPT-11; 7-ethyl-10-[4-(1-piperidino)-1-piperidino]carbonyloxycamptothecin[4-6]), capecitabine[7], oseltamivir[8], lidocaine[9] and meperidine[10]). The prevalence of the ester function in these latter molecules is partly due to the fact that this chemotype improves water solubility and bioavailability of these compounds. Hence for the development of new drugs from chemical screens that are poorly water soluble, it is highly likely that medicinal chemists would develop ester, carbamate or amide derivatives that would result in compounds that may be substrates for CEs.

The impact of CEs on drug metabolism has been demonstrated both with regard to toxicity and antitumor activity. For example, plasma-esterase deficient mice are more resistant to the toxic effects of irinotecan due to reduced conversion to the toxic metabolite 7-ethyl-10-hydroxycamptothecin (SN-38).[11] Conversely, tumor cells that express CEs are more sensitive to this agent since enhanced drug hydrolysis occurs, resulting in higher intracellular concentrations of 7-ethyl-10-hydroxycamptothecin and as a consequence, more cytotoxicity.[12] Clearly therefore, the levels of CE are important with respect to these sequelae. We have determined that molecules containing the ethane-1,2-dione moiety can be

potent inhibitors of human CEs and these compounds can significantly modulate the hydrolysis of esterified agents.[13] More recently, we have searched natural product databases with a defined pharmacophore (containing the structural and electronic components of the ethane-1,2-dione chemotype) and identified the tanshinones as highly effective CE inhibitors.[14] These compounds modulate enzyme activity in vitro and the cytotoxic effects of irinotecan in cell culture models. The tanshinones are present in high quantities in Danshen root, a herbal medicine widely used in China, and this is currently being used in clinical trials in the US as Compound Danshen Dripping Pill. Potentially therefore, the metabolism of esterified agents may be impacted in individuals using this material.

The tanshinones are all pan CE inhibitors, modulating activity of both the human liver isoform (hCE1; CES1) and the intestinal enzyme (hiCE; CES2). Hence while these are important reagents for biochemical studies, they do not allow discrimination of CE-mediated ester hydrolysis in complex samples.

Based upon our observations, we have furthered our initial database searches and evaluated the presence of the ethane-1,2-dione moiety in other natural products. This identified β-lapachone (ARQ501; **1**)[15] as a candidate molecule and results described here demonstrate that this compound, and selected derivatives thereof, are potent human CE inhibitors, both in vitro, and in cell culture models. Based upon this information, we have developed isozyme selective compounds that specifically inhibit hCE1.[16]

RESULTS AND DISCUSSION

Identification of 1 as a carboxylesterase inhibitor

We have previously reported that the ethane-1,2-dione moiety, when present within a hydrophobic scaffold, can act as a potent inhibitor of CEs.[13, 17-20] This has been demonstrated for a series of tanshinones[14] and we have confirmed that Chinese herbal medicines that contain these molecules can modulate esterified drug metabolism. Since such medicines are widely used, we sought to examine whether other natural products might contain structurally similar compounds and if so, whether they harbored biological activity towards human CEs. Therefore using a esterase inhibitor pharmacophore that we have previously defined[14], we identified **1** (Figure 1) as a potential candidate molecule.

Since this compound is readily available, we determined the ability of **1** to inhibit human CEs. As indicated in Table 1, when using o-nitrophenyl acetate (o-NPA) as a substrate, this molecule was a reasonable inhibitor of hiCE (K_i = 109 nM), although considerably less active (~10-fold) towards hCE1. Indeed, the potency of **1** was similar to that seen for other 1,2-diones (cf. 14 nM and 45 nM for benzil with hiCE and hCE1, respectively[13]; 118 nM and 398 nM for dihydrotanshinone with hiCE and hCE1, respectively[14]). However as these concentrations are lower than that required for **1** to induce cytotoxicity in cultured cells in vitro[21-23], this suggests that modulation of CE activity likely occurs under these circumstances. We advise caution therefore, when using this compound in conjunction with esterified agents that might be activated (e.g., irinotecan) or inactivated by these enzymes. Based upon this information, we sought to characterize the ability of analogues of **1** to inhibit human CEs.

Synthesis of 4-substituted 4-phenoxynaphthalene-, 4-(phenylamino)naphthalene-, and 4-phenyl(methyl)amino naphthalene-1,2-diones

Using a simple one step synthetic approach[24], we generated a library of phenoxy, phenylamino and phenyl-N-methylamino analogues in reasonable yields, which differed only in the substituent at the 4-position of the free phenyl ring (H, MeO, Me, F, Cl, Br, I). In all cases, synthesis readily occurred to yield either yellow (phenoxy) or dark red (phenyl amino and phenyl(methyl)amino) solids. Following physical characterization and confirmation of identity (see Supporting Information), the ability of these compounds to inhibit human CEs was assessed.

Inhibition of human CEs by 4-substituted 4-phenoxynaphthalene-1,2-diones

All phenoxynaphthalene-1,2-diones were potent inhibitors of both hCE1 and hiCE when using o-NPA as a substrate, although the K_i values were 4- to 11-fold lower for the former enzyme (Table 2). This contrasts the activity of **1** which is ~10-fold more active towards hiCE. A trend was observed such that the more hydrophobic compounds (i.e., those with greater logP values) were more potent enzyme inhibitors (data not shown). It should be noted, that in general, all of the 4-phenoxynaphthalene-1,2-diones were more active than **1**, and that none of these compounds demonstrated any appreciable activity towards human acetylcholinesterase (AChE; Table 2). All compounds acted in a partially competitive fashion with respect to the mode of enzyme inhibition, i.e., while they act in a competitive manner, they are unable to completely inhibit product formation at infinite inhibitor concentrations.[25] This is similar to results obtained using the benzils and the tanshinones.[13, 14]

Inhibition of human CEs by 4-substituted 4-(phenylamino)naphthalene-1,2-diones

In contrast to that seen for 4-phenoxynaphthalene-1,2-diones, essentially all of the phenylamino derivatives (compounds **9**-**15**) were inactive towards both human enzymes (Table 2). Indeed, the maximal inhibition observed at an inhibitor concentration of 10 μM was 41% for 4-[(4-iodophenyl)amino]naphthalene-1,2-dione (**15**) with hCE1. To determine if there were any structural or molecular interactions that might account for the lack of enzyme inhibition by the amino derivatives, we docked 3 of each class of compounds (molecules **2**, **3** and **6**, and **9**, **10** and **13**) into the active site of the crystal structure of hCE1. This was achieved using Molsoft ICM software using the default parameters for small ligand docking. As indicated in Figure 2, all of the small molecules were juxtaposed adjacent to the active site serine in an identical conformation to that seen for compound **1**. In addition, virtually no differences were observed in the distances from the Oγ atom of the amino acid to the carbonyl carbon atoms of the docked compounds (distances ranged from 3.03Å to 3.26Å). In general, the ICM scores for docking of the small molecules were comparable (see Figure 2 legend), although all of the values obtained for the phenoxy derivatives (compounds **2**, **3** and **6**) were lower than that seen for the respective aniline. Since the mechanism of enzyme inhibition is believed to be due to a coordinated attack by the serine Oγ atom on one of the carbonyl carbon atoms within the the 1,2-dione moiety, it is unlikely that the loss of activity of the phenylamino derivatives is due to poor access or localization within the enzyme active site.

Since previous reports have indicated that phenylaminonaphthalene-1,2-diones can undergo tautomerism resulting in loss of the 1,2-dione moiety (see Figure 3a)[26-28], we assessed whether the imino forms would dock in a similar fashion as the phenoxy analogues. As can be seen (Figure 3c), the carbon atom attached to the hydroxyl group was proximal to the serine Oγ atom in compound **9**, with the carbonyl carbon up to 4.45Å from this residue. Similar results were obtained from docking the imino tautomers of the other phenylaminonaphthalene-1,2-diones (data not shown). Previous studies using a panel of benzoins and corresponding benzils[13, 17] have yielded similar results, but it has not been possible to undertake simple chemical modifications of these molecules to specifically address the role of the hydroxyl/carbonyl carbon atom configuration with respect to CE inhibition. We postulated therefore that it is unlikely that the imino compounds would act as inhibitors since the carbonyl carbon atom is not adjacent to the serine Oγ atom.

Inhibition of human CEs by 4-substituted phenyl (methyl)aminonaphthalene-1,2-diones

To limit the amino-imino tautomerism of the 4-(phenylamino)naphthalene-1,2-diones, we synthesized a similar panel of N-methylated aniline analogues (compounds **12**-**22**) using the same methods, and evaluated whether they would act as CE inhibitors. We hypothesized that methylating the nitrogen atom would prevent formation of the imino moiety due to the lack of the labile amine hydrogen atom. As indicated in Table 2, all of the N-methyl substituted compounds, with the exception of the iodo analogue (**22**), were potent inhibitors of hCE1 with K_i values comparable to that seen for the phenoxy analogues (Table 1). Indeed, the most potent compound, (the bromo derivative; **21**)

demonstrated an inhibition constant of ~16 nM. These data further support the hypothesis that the loss of the 1,2-dione in the phenylaminonaphthalene-1,2-diones, via tautomerism to the imino form (Figures 3a and 3b), significantly compromises enzyme inhibitory activity of the former.

When we docked compound **16** into the active site of hCE1, the docking pose demonstrated a significant difference in the distance of the serine Oγ atom to the closest carbonyl atom, as compared to the imino form of **9** (Figures 3c and d). For the latter compound, the distance is 4.45Å, whereas for the N-methylated analogue, this value is 3.08Å. It should also be noted that with the imino form, the OH group is juxtaposed closest to the catalytic serine Oγ atom. Since esterases do not attack alcohol bonded carbon atoms, these docking studies provide further support for the lack of activity of the phenyl aniline derivatives.

Interestingly, the N-methylated aniline analogues with smaller, less hydrophobic substituents demonstrated selectivity for hCE1, with little or no activity towards hiCE at concentration up to 10μM (Table 2). Compound **21** was weakly active towards hiCE (53% inhibition at 10 μM), whereas **22** was moderately potent towards both human CEs. The mechanism to account for this selectivity is not understood since we do not believe that any electronic effects could be responsible for the loss of activity. Potentially, the architecture of the hiCE active site may be sufficiently different from hCE1 such that steric hinderance may influence CE inhibitor binding. However, since the crystal structure of hiCE has not been determined, and this enzyme is very labile[29], an analysis of the

interaction of the phenyl (methyl)aminonaphthalene-1,2-diones with this enzyme may require other physical approaches (e.g., NMR, SPR, etc).

Compound **22**, which contains an iodine atom at the 4-position of the free phenyl ring, was considerably less active that the other analogues (K_i with hCE1 = 400nM; Table 2). However, docking of this molecule into the active site of this protein demonstrated no difference in the alignment as compared to the other N-methyl analogues that were potent inhibitors (data not shown). Indeed, the distance between the serine Oγ and the carbonyl carbon atoms was measured at 3.01 Å and 3.28Å for **22**. However, we have previously demonstrated that for hCE1, the amino acids forming the entrance to the active site gorge are relatively immobile, limiting substrate access to the catalytic residues.[29] We hypothesize therefore, that **22** is unable to freely enter the enzyme active site due to the increased size of the iodo atom, relative to the substituents in the other phenyl(methyl)amino derivatives. As a consequence, the K_i value for hCE1 inhibition by the iodo derivative is larger (i.e. the molecule is less potent). Since the active site in hiCE is more plastic and can readily accept larger substrates than hCE1,[3, 29] **22** demonstrates modest activity towards the former enzyme, likely due to its ability to access the catalytic serine residue. In toto, these results argue that the biological activity of **22** is modulated by the relative size of the molecule and its ability to enter the active site and interact with the catalytic amino acids within the human CEs.

Assessment of imine formation in phenylaminonaphthalene-1,2-diones

To confirm that imine formation was the likely reason for the loss of activity of the phenylaminonaphthalene-1,2-diones, we undertook three different approaches to assess the presence of this chemotype in these molecules. Firstly, the crystal structures of compounds **2**, **9** and **16**, as well as 1,2-naphthoquinone (**23**) were determined, and the lengths of relevant bonds were assessed. We also compared these results with those obtained from structurally similar molecules (4-amino-1,2-naphthquinone (**24**) and 4-(9H-carbazol-9-yl)-1,2-naphthoquinone (**25**)) that had previously been crystalized. We hypothesized that in compounds that would could undergo the amino-imino tautomerization, the C-N bond between the 1,2-dione-containing ring and the heteroatom would be shorter in length due to the formation of the double bond.

As can be seen in Figure 4, the C-N bond in **9** is shorter than that seen in the N-methyl derivative **16** (1.352 Å versus 1.374 Å), and considerably smaller than that observed in the carbazoyl analogue **25** (1.411 Å). In addition, this bond length in **9,** is longer than that observed in the unsubstituted 4-amino-1,2-naphthoquinone (**24**). Since compounds **24** and **25** represent molecules which would be the most likely and unlikely to undergo imine formation, respectively, these results suggest that the C-N bond in **9** likely has partial double bond character.

Further support for this tautomerization was provided by examining the C-C and the C=O bonds in the respective analogues (bonds 2, 3 and 4 in Figure 4). In **2**, **16**, **23**, and **25**, the C-C bond (bond 2) is shorter than that observed for molecules **9** and **24**, consistent with the hypothesis that this is likely to exist as a

single bond in the latter two molecules. In contrast, bond 3 is shorter in **9** and **24** as compared to the other compounds, suggesting that it exhibits more double bond character in these molecules. Furthermore, the C=O bond (bond 4 in Figure 4) is shorter in the compounds that would be unlikely to undergo imine formation (i.e., **2**, **16**, **23**, and **25**), but considerably longer in **9** and **24**. Overall, these structural studies argue that **9** and **24** maintain more imine-like character than the other molecules analyzed.

Since the crystallographic studies obviously evaluated bond distances in the solid state which may not be entirely reflective of what occurs in solution, we used NMR to determine the structures of naphthalene-1,2-dione analogues under different solvent conditions. While the ^{1}H and ^{13}C spectra for compounds **2** and **16**, when dissolved in DMSO, were readily interpretable, the data obtained for **9** contained multiple overlapping peaks and were difficult to assign (see Supporting Information). Since we presumed that this was due to the presence of the two different tautomers in the sample, we opted to simplify the analyses and to evaluate the ^{19}F NMR signals using the fluorinated derivatives (compounds **5**, **12** and **19** for the phenol, the aniline and the N-methylaniline analogues, respectively). As indicated in Figure 5 (panels a and e), single peaks were observed for **5** (115.77ppm) and **19** (116.32ppm), corresponding to the fluorine atom in the para position of the appended benzene ring. However, the aniline (**12**) yielded two signals at 114.97ppm and 119.80ppm (Figure 5c), likely due to the presence of the amino and imino tautomers within the sample. Consistent with this hypothesis, the inclusion of base (triethylamine) into the latter sample, yielded a spectrum containing a broad single peak (116.93ppm), likely resulting

from an increase in the rate of interconversion of the imine to the amine (see Figure 5d). Base would facilitate this process by abstraction of the labile proton in this structure. Since the shift of the signal peak was very similar to the singlet seen for **19** in DMSO, we believe that under basic conditions **12** exists primarily in its amino form.

To confirm the results seen in organic solvent, we used UV spectroscopy to assess the changes in absorption of the molecules in aqueous solutions (20% DMSO:80% 200 mM sodium phosphate buffer) at different pH values. Little, if any, change was observed in the spectra for compounds **2** and **16** over the pH3-11 range (Figures 5g and 5j), consistent with the hypothesis that these molecules do not change structure in these acidic/basic environments. In contrast, compound **9** ((4-phenylamino)naphthalene-1,2-dione), demonstrated significant changes in the UV spectrum over the pH range used (Figure 5h). Under neutral or acidic conditions, the spectra were essentially identical with a peak maxima at 475 nm. However at pH9 and pH11 this maxima was shifted to lower wavelengths of 461 and 453 nm, respectively. This hypsochromic shift is consistent with a decrease in conjugation of **9** due the loss of the double bond between the nitrogen atom and the aliphatic ring (bond 1 in Figure 4), i.e., by conversion from the imine to the amine. Since no changes in the spectra were observed for compounds **2** and **16** over these pH ranges, we conclude that this tautomerization does not occur under these conditions for these molecules. Overall, these crystallographic, NMR and UV spectral analyses indicate that compound **9** likely exists in tautomeric forms that include the imine and amine. This is not observed with either the phenoxy (**2**), fluorophenoxy (**5**), N-

methylamino (**16**) or 4-fluorophenyl N-methylamino (**19**) derivatives. Since the imino tautomers would be very unlikely to act as CE inhibitors (due to the loss of the 1,2-dione moiety), our data is strongly supportive of the hypothesis that the lack of biological activity of the amines is due to the presence of this tautomerization.

Inhibition of oseltamivir and irinotecan hydrolysis by β-lapachone analogues

Having demonstrated inhibition of CEs in vitro by the naphthalene-1,2-diones, we assessed whether these molecules were membrane permeable and could modulate drug metabolism in cultured cells. Two different drugs were used as substrates since they are selectively hydrolyzed by different human CEs: hCE1 for oseltamivir; and hiCE for irinotecan. As indicated in Figure 6a, **1** and the phenoxy analogues (**2**-**7**) were reasonable inhibitors of hCE1, yielding anywhere from a 12-47% reduction of metabolite formation. However, the phenyl(methyl)amino derivatives (**16**-**21**) were considerably more potent (Figure 6b) resulting in significant loss of oseltamivir carboxylate production (up to 99% with compound **19**), confirming that these molecules can inhibit hCE1 intracellularly.

Interestingly, while **1** was an excellent inhibitor of hiCE in cells (as indicated by the greater than 90% loss in 7-ethyl-10-hydroxycamptothecin production; Figure 6c), the 4-phenoxynaphthalene-1,2-diones (**2**-**7**) were essentially inactive in this assay. This contrasts with the in vitro results, although it should be noted that these compounds are 5- to 10-fold less active towards hiCE as compared to hCE1 (Table 1). Consistent with the in vitro assays, compounds **16**-**21** yielded

very little inhibition of hiCE (Figure 6d). Overall, these results confirm the in vitro selectivity of the N-methyl amino derivatives towards hCE1, and demonstrate the cell permeability of these compounds.

To date, the identification of the specific CEs responsible for drug activation in humans has been problematic, in part due to lack of specific reagents to assess such reactions. For example, there are no specific hCE1 inhibitors and/or simple chromogenic substrates that can be used for rapid biochemical analyses. We have generated benzene sulfonamides as selective hiCE modulators[30] and have tried to use these in combination with pan CE inhibitors (e.g., benzils[13]) to assess esterified substrate hydrolysis in complex samples.[31] While partially successful, due to the numerous esterases present within mammalian tissues and microsomes, definitive results require the use of time-consuming and labor-intensive chromatographic purification. However, based upon the data presented here, we propose that either compound **17** or **18** would be the best choice for use in reaction profiling of complex biological samples with respect to CE-mediated drug hydrolysis. These molecules exhibit potency towards hCE1 (K_i values of ~80 and 11 nM, respectively), yet at 10 μM, only demonstrate 7% and 25% inhibition of hiCE (Table 2). In cell based studies, both compounds were potent and selective, yielding greater than 94% inhibition of hCE1 and less than 23% inhibition of hiCE (Figure 6). Used in combination with benzene sulfonamides[32], benzils[13], and total esterase inhibitors (e.g. bis-(4-nitrophenyl) phosphate), these compounds will allow studies to document hCE1-specific substrate metabolism in complex enzyme mixtures.

Since *o*-quinones are known to be cytotoxic, we determined U373MG cell viabilities after 30 min exposure (the time period used for the cellular enzyme inhibition studies), and growth inhibition after 72 hr dosing, for selected N-methylaniline analogues. Short term assays indicated no obvious effects, with cell viabilities of 99 ± 6%, 100 ± 14% and 96 ± 5% being recorded for **16**, **18** and **19**, respectively. In longer term assays (72 hr), these molecules yielded IC_{50} values of 12.8 ± 5.8 μM, 4.6 ± 1.1 μM, and 3.9 ± 1.0 μM, respectively (see Supporting Information). The latter data suggest that these compounds do exert cytotoxic effects, but these only occur over an extended time frame. Since enzyme inhibition studies typically involve incubations of less than 1 hr, the effects of these inhibitors with regard to cell toxicity would be minimal and can essentially be discounted.

CONCLUSIONS

In summary, we have determined that **1** is a potent inhibitor of human CEs and this occurs at concentrations lower than that required to induce cytotoxicity.[21-23] Typically 1-5 μM is required for the latter, whereas the K_i values for **1** with purified hCE1 or hiCE are 1.2 and 0.1 μM respectively. Since 11 different clinical trials with **1** are noted in Clinicaltrials.gov, studies must be designed cautiously to ensure that this compound is not combined with agents that might be activated (e.g., irinotecan) or inactivated by these enzymes. Additionally, our studies have identified potent, selective hCE1 inhibitors based upon the β-lapachone scaffold. This is the first report of such compounds and these molecules will now allow for a detailed evaluation of drug metabolism by samples containing multiple human

CEs. Hence, reaction profiling of complex enzyme mixtures (e.g., tissue samples, microsomes, cell extracts, etc.) using a combination of specific CE inhibitors will allow for rapid identification of target enzymes. Such studies are currently underway.

EXPERIMENTAL SECTION

Materials and general procedures

1 was purchased from Sigma Aldrich (St. Louis, MO) and was used without purification. Pure hCE1 and hiCE were generated by expressing the respective cDNAs in *Spodoptera frugiperda* Sf9 cells using baculoviral vectors. Secreted, active enzyme was purified from serum-free culture media using preparative isoelectric focusing and chromatography.[3, 33] Human AChE was purchased from Sigma Biochemicals (St. Louis, MO). U373MG cells expressing hCE1 or hiCE have been previously described.[34]

Reagents for chemical synthesis were purchased from Sigma Aldrich (St. Louis, MO) or Oakwood Products (Estill, SC) and were used without further purification. Reactions were typically carried out at a 10mmole scale and analyzed using a Waters Acquity UPLC with an SQ Detector 2 (UV, ELSD, MS). Purification of products was achieved using a Biotage ACI flash chromatography system with Biotage SNAP Ultra HP-Sphere 25 μM 10g columns or a Waters Prep LC 4000 with Waters symmetry C18 column 19 X 300 mm. Overall yields were in the 20-40% range. Typically, crude material was dissolved in a minimal amount of DMSO and applied to the column. Compounds were then eluted using a 10-100% hexane/ethyl acetate gradient over 20 min at a flow rate of 35 ml/min. Solvent from purified fractions was then removed under reduced pressure and the identity of isolated molecules confirmed using ^{1}H and ^{13}C NMR, and HRMS. All compounds were deemed to be greater than 95% pure using analytical UPLC-MS analysis and NMR.

NMR spectra were obtained in either DMSO-d_6 or $CDCl_3$ using a 500 MHz Bruker Avance spectrometer equipped with XH dual probe. Chemical shifts are reported based upon TMS or fluorobenzene as a standard. HRMS were determined with a Waters Acquity UPLC – Xevo G2 QTOF spectrometer.

The atom coordinates for compounds **24** and **25**, AMNPQH10 and XANRUB, respectively, were obtained from the CSD database and analyzed using Mercury software.

Chemical synthesis

*General methods for 4-substituted 4-phenoxynaphthalene-1,2-diones (**2**-**8**)*

4-Substituted 4-phenoxynaphthalene-1,2-diones were synthesized by condensation of the corresponding phenol (5.5 mmol) with sodium 3,4-dioxo-3,4-dihydronaphthalene-1-sulfonate (5 mmol).[24] Reactions were conducted in 150ml of water containing KOH (5 mmol). After solvent removal, the dried residue was subjected to flash chromatography, preparative HPLC, and in some cases, recrystallization from ethanol, to afford yellow solids. The synthesis of compounds **2**, **3** and **6** have been previously reported and their chemical parameters are included in the Supporting Information.[24, 35] The physical and chemical properties of novel molecules are listed here.

*4-(4-Methylphenoxy)naphthalene-1,2-dione (**4**)*

Compound **4** was synthesized according to the general method using 4-methylphenol as the starting material. This yielded a yellow solid (53 mg, 28%). Mp 165 ºC; UV-Vis λ_{max}: 250 nm, 280 nm, 326 nm, and 403 nm in methanol. ^{1}H NMR (400 MHz, $CDCl_3$) δ 8.16 (dd, *J* = 1.4, 7.7 Hz, 1H), 8.09 (dd, *J* = 1.2, 7.8 Hz, 1H), 7.77 (td, *J* = 1.5, 7.7 Hz, 1H), 7.65 (td, *J* = 1.3, 7.6 Hz, 1H), 7.31 – 7.23 (m,

2H), 7.09 – 6.99 (m, 2H), 5.67 (s, 1H), 2.40 (s, 3H). ^{13}C NMR (101 MHz, $CDCl_3$) δ 179.55, 179.38, 169.02, 150.12, 136.78, 135.10, 131.85, 131.72, 130.81 (2C), 130.50, 129.34, 124.92, 120.93 (2C), 106.32, 20.91. HRMS (ESI): *m/z* 265.0873 (M + H) (calcd for $C_{17}H_{12}O_3$, 265.0864) (M + H).

*4-(4-Fluorophenoxy)naphthalene-1,2-dione (**5**)*

Compound **5** was synthesized according to the general method using 4-fluorophenol as the starting material. This yielded a yellow solid (80 mg, 37%). Mp 190 ºC; UV-Vis λ_{max}: 250 nm, 320 nm, and 398 nm in methanol. ^{1}H NMR (500 MHz, $CDCl_3$) δ 8.18 (dd, *J* = 1.3, 7.7 Hz, 1H), 8.08 (dd, *J* = 1.1, 7.9 Hz, 1H), 7.78 (td, *J* = 1.4, 7.7 Hz, 1H), 7.67 (td, *J* = 1.2, 7.6 Hz, 1H), 7.23 – 7.12 (m, 4H), 5.64 (s, 1H). ^{13}C NMR (126 MHz, $CDCl_3$) δ 179.46, 179.11, 168.78, 161.77, 159.81, 148.11, 135.17, 132.02, 131.42, 130.46, 129.51, 124.87, 122.87, 117.28, 117.10, 106.33. ^{19}F NMR (471 MHz, DMSO) δ -115.77. HRMS (ESI): *m/z* 269.0614 (M + H) (calcd for $C_{16}H_9FO_3$, 269.0611) (M + H).

*4-(4-Bromophenoxy)naphthalene-1,2-dione (**7**)*

Compound **7** was synthesized according to the general method using 4-bromophenol as the starting material. This yielded a yellow solid (63 mg, 24%). Mp 210 ºC; UV-Vis λ_{max}: 250 nm, 278 nm, 328 nm, and 397 nm in methanol. ^{1}H NMR (500 MHz, $CDCl_3$) δ 8.21 – 8.15 (m, 1H), 8.07 (dd, *J* = 1.2, 7.8 Hz, 1H), 7.78 (td, *J* = 1.4, 7.6 Hz, 1H), 7.67 (td, *J* = 1.2, 7.6 Hz, 1H), 7.65 – 7.58 (m, 2H), 7.11 – 7.04 (m, 2H), 5.65 (s, 1H). ^{13}C NMR (126 MHz, $CDCl_3$) δ 179.40, 179.02, 168.36, 151.34, 135.18, 133.54 (2C), 132.07, 131.34, 130.46, 129.55, 124.87, 123.14 (2C), 120.21, 106.44. HRMS (ESI): *m/z* 328.9810 (M + H) (calcd for $C_{16}H_9BrO_3$, 328.9813) (M + H).

*4-(4-Iodophenoxy)naphthalene-1,2-dione (**8**)*

Compound **8** was synthesized according to the general method using 4-Iodophenol as the starting material. This yielded an orange solid (132 mg, 44%). Mp 220 ºC; UV-Vis λ_{max}: 247 nm, 274 nm, 329 nm, and 397 nm in methanol. ^{1}H NMR (500 MHz, $CDCl_3$) δ 8.21 (dd, *J* = 1.3, 7.6 Hz, 1H), 8.08 (dd, *J* = 1.1, 7.8 Hz, 1H), 7.87 – 7.76 (m, 3H), 7.69 (td, *J* = 1.2, 7.6 Hz, 1H), 7.00 – 6.93 (m, 2H), 5.68 (s, 1H). ^{13}C NMR (126 MHz, $CDCl_3$) δ 179.40, 179.04, 168.34, 152.19, 139.55 (2C), 135.18, 132.07, 131.36, 130.47, 129.56, 124.88, 123.48 (2C), 106.47, 91.07. HRMS (ESI): *m/z* 376.9671 (M + H) (calcd for $C_{16}H_9IO_3$, 376.9675) (M + H).

*General methods for 4-substituted (4-phenylamine)naphthalene-1,2-diones (**9**-**15**)*

4-Substituted (4-phenylamine)naphthalene-1,2-diones were synthesized by condensation of the corresponding aniline (5.5 mmol) with sodium 3,4-dioxo-3,4-dihydronaphthalene-1-sulfonate (5 mmol).[24] Syntheses were conducted in 150 ml of water and after solvent removal, the products were purified using flash chromatography, to generate red solids. The synthesis of compounds **9**-**14** have been previously reported and their physical parameters are reported in the Supporting Information.[24, 27, 28, 36, 37]

*4-((4-Iodophenyl)amino)naphthalene-1,2-dione (**15**)*

Compound **15** was synthesized according to the general method using 4-iodoaniline as the starting material. This yielded a red solid (148 mg, 78%). Mp 262 ºC; UV-Vis λ_{max}: 280 nm, 340 nm and 456 nm in methanol. ^{1}H NMR (500 MHz, DMSO) δ 8.32 (d, *J* = 7.9 Hz, 1H), 8.03 (dd, *J* = 1.4, 7.8 Hz, 1H), 7.82 (dd,

J = 7.0, 8.4 Hz, 1H), 7.74 (m, 4H), 6.94 (d, *J* = 8.1 Hz, 2H), 5.88 (s, 1H). ^{13}C NMR (126 MHz, DMSO) δ 182.24, 155.71, 148.96, 138.28, 137.53, 134.08, 133.48, 131.66, 131.59, 127.31, 124.86, 116.96, 102.14, 76.15. HRMS (ESI): *m/z* 375.9838 (M + H) (calcd for $C_{17}H_{12}NIO_2$, 375.9834) (M + H).

*General methods for 4-substituted (4-phenyl(methyl)amine)naphthalene-1,2-diones (**16**-**22**)*

4-Substituted (4-phenyl(methyl)amine)naphthalene-1,2-diones were synthesized in an identical fashion to that described for the (4-phenylamine)naphthalene-1,2-diones (see above) to afford red solids. The synthesis of compound **16** has been previously reported and its physical parameters are reported in the Supporting Information.[28]

*4-((4-Methoxyphenyl)(methyl)amino)naphthalene-1,2-dione (**17**)*

Compound **17** was synthesized according to the general method using 4-methoxy-N-methylaniline as the starting material. This yielded a red solid (59 mg, 40%). Mp 167 ºC; UV-Vis λ_{max}: 280 nm, 383 nm, and 483 nm in methanol. ^{1}H NMR (500 MHz, CDCl3) δ 8.07 (dd, J = 1.5, 7.6 Hz, 1H), 7.35 (td, J = 1.0, 7.5 Hz, 1H), 7.24 (td, J = 1.6, 7.8 Hz, 1H), 7.08 – 7.01 (m, 3H), 6.90 – 6.83 (m, 2H), 6.25 (s, 1H), 3.80 (s, 3H), 3.46 (s, 3H). ^{13}C NMR (126 MHz, CDCl3) δ 181.04, 178.29, 159.36, 158.12, 140.75, 133.25, 132.69, 132.24, 129.90, 129.01, 128.89, 126.72 (2C), 115.18 (2C), 109.83, 55.54, 44.62. HRMS (ESI): *m/z* 294.1129 (M + H) (calcd for $C_{18}H_{15}NO_3$, 294.1130) (M + H).

*4-((4-Methylphenyl)(methyl)amino)naphthalene-1,2-dione (**18**)*

Compound **18** was synthesized according to the general method using 4-methyl-N-methylaniline as the starting material. This yielded a red solid (35 mg, 25%).

Mp 140 ºC; UV-Vis λ_{max}: 274 nm, 320 nm, 376 nm, and 467 nm in methanol. ^{1}H NMR (500 MHz, $CDCl_3$) δ 8.08 (dd, *J* = 1.5, 7.8 Hz, 1H), 7.35 (td, *J* = 1.1, 7.5 Hz, 1H), 7.29 – 7.19 (m, 1H), 7.18 – 7.10 (m, 2H), 7.09 – 6.96 (m, 3H), 6.27 (s, 1H), 3.47 (s, 3H), 2.34 (s, 3H). ^{13}C NMR (126 MHz, $CDCl_3$) δ 180.96, 178.43, 159.54, 145.34, 136.57, 133.25, 132.74, 132.19, 130.58 (2C), 129.95, 129.06, 128.90, 125.32 (2C), 110.39, 44.40, 20.99. HRMS (ESI): *m/z* 278.1180 (M + H) (calcd for $C_{18}H_{15}NO_2$, 278.1181) (M + H).

*4-((4-Fluorophenyl)(methyl)amino)naphthalene-1,2-dione (**19**)*

Compound **19** was synthesized according to the general method using 4-fluoro-N-methylaniline as the starting material. This yielded a red solid (44 mg, 31%). Mp 190 ºC; UV-Vis λ_{max}: 272 nm, 320 nm, 370 nm, and 461 nm in methanol. ^{1}H NMR (500 MHz, CDCl3) δ 8.09 (dd, J = 1.5, 7.7 Hz, 1H), 7.38 (td, J = 1.1, 7.6 Hz, 1H), 7.27 (td, J = 1.5, 7.8 Hz, 1H), 7.15 – 7.05 (m, 2H), 7.09 – 7.00 (m, 3H), 6.28 (s, 1H), 3.47 (s, 3H). ^{13}C NMR (126 MHz, $CDCl_3$) δ 180.59, 178.57, 160.67 (d, *J* = 248.0 Hz), 159.41, 143.98, 133.43, 132.45, 132.14, 130.17, 129.31, 128.73, 126.95 (d, *J* = 8.5 Hz)(2C), 116.96 (d, *J* = 23.1 Hz)(2C), 111.00, 44.48. HRMS (ESI): *m/z* 282.0934 (M + H) (calcd for $C_{17}H_{12}FNO_2$, 282.0930) (M + H).

*4-((4-Chlorophenyl)(methyl)amino)naphthalene-1,2-dione (**20**)*

Compound **20** was synthesized according to the general method using 4-chloro-N-methylaniline as the starting material. This yielded a red solid (88 mg, 59%). Mp 182 ºC; UV-Vis λ_{max}: 245 nm, 275 nm, 320 nm, 373 nm, and 462 nm in methanol. ^{1}H NMR (500 MHz, $CDCl_3$) δ 8.08 (dd, *J* = 1.5, 7.6 Hz, 1H), 7.39 (td, *J* = 1.1, 7.5 Hz, 1H), 7.31 (m, 3H), 7.06 (m, 3H), 6.29 (s, 1H), 3.48 (s, 3H). ^{13}C NMR (126 MHz, $CDCl_3$) δ 180.44, 178.67, 159.27, 146.38, 133.60, 132.40,

132.02, 131.76, 130.24, 130.08 (2C), 129.32, 128.70, 126.33 (2C), 111.76, 44.06. HRMS (ESI): *m/z* 298.0636 (M + H) (calcd for $C_{17}H_{12}ClNO_2$, 298.0635) (M + H).

*4-((4-Bromophenyl)(methyl)amino)naphthalene-1,2-dione (**21**)*

Compound **21** was synthesized according to the general method using 4-bromo-N-methylaniline as the starting material. This yielded a red solid (62 mg, 36%). Mp 182 ºC; UV-Vis λ_{max}: 246 nm, 319 nm, 365 nm and 463 nm in methanol. ^{1}H NMR (500 MHz, $CDCl_3$) δ 8.07 (dd, *J* = 1.4, 7.7 Hz, 1H), 7.46 (m, 2H), 7.39 (td, *J* = 1.0, 7.5 Hz, 1H), 7.30 (m, 1H), 7.04 (m, 3H), 6.29 (s, 1H), 3.48 (s, 3H). ^{13}C NMR (126 MHz, $CDCl_3$) δ 180.40, 178.67, 159.22, 146.85, 133.63, 133.02 (2C), 132.36, 131.99, 130.24, 129.31, 128.68, 126.61 (2C), 119.48, 111.90, 43.96. HRMS (ESI): *m/z* 342.0127 (M + H) (calcd for $C_{17}H_{12}BrNO_2$, 342.0129) (M + H).

*4-((4-Iodophenyl)(methyl)amino)naphthalene-1,2-dione (**22**)*

Compound **22** was synthesized according to the general method using 4-iodo-N-methylaniline as the starting material. This yielded a red solid (74 mg, 38%). Mp 184 ºC; UV-Vis λ_{max}: 270 nm, 316 nm, and 452 nm in methanol. ^{1}H NMR (500 MHz, $CDCl_3$) δ 8.10 (dd, *J* = 1.4, 7.6 Hz, 1H), 7.65 (m, 2H), 7.40 (td, *J* = 1.1, 7.5 Hz, 1H), 7.31 (td, *J* = 1.5, 7.8 Hz, 1H), 7.05 (d, *J* = 8.1 Hz, 1H), 6.86 (m, 2H), 6.30 (s, 1H), 3.47 (s, 3H). ^{13}C NMR (126 MHz, $CDCl_3$) δ 180.38, 178.76, 159.20, 147.58, 139.00 (2C), 133.66, 132.40, 132.03, 130.29, 129.42, 128.65, 126.82 (2C), 112.18, 90.35, 43.88. HRMS (ESI): *m/z* 389.9990 (M + H) (calcd for $C_{17}H_{12}INO_2$, 389.9991) (M + H).

1,2-Naphthoquinone (**23**)

Compound **23** was synthesized as previously described[16], and purified by sublimation to yield orange plate-like crystals. Physical parameters for this molecule are provided in the Supporting Information.

Enzyme inhibition assays

The inhibition of CE-mediated o-nitrophenyl acetate (o-NPA) and oseltamivir hydrolysis by the 1,2-diones was performed as previously described.[32] Routinely all data points were performed in quadruplicate, with at least 8 different concentrations of inhibitor. Analysis of results was undertaken by fitting data to the following equation to determine the mode of enzyme inhibition:[24]

$$i = \frac{[I]\{[s](1-\beta) + Ks(\alpha - \beta)\}}{[I]\{[s] + \alpha Ks\} + Ki\{\alpha[s] + \alpha Ks\}}$$

where *i* = fractional inhibition, [*I*] = inhibitor concentration, [*s*] = substrate concentration, α = change in affinity of substrate for enzyme, β = change in the rate of enzyme substrate complex decomposition, *Ks* is the dissociation constant for the enzyme substrate complex and *Ki* is the inhibitor constant. GraphPad Prism software was used to evaluate the curve fits where α ranged from 0 to ∞ and β from 0 to 1. Those generating the highest r^2 values were then analyzed using Akaike's information criteria[38, 39] to identify the best model for enzyme inhibition. K_i values for enzyme inhibition were then calculated from the equation predicted by Prism to be the best fit for the experimental data.[32]

Inhibition of human AChE was assessed using a spectrophotometric assay with acetylthiocholine (ATCh) as a substrate.[40]

Small molecule docking

Small molecules were drawn, optimized and docked into the hCE1 enzyme active site (RCSB code 1MX1) using ICM Pro software (Molsoft LLC, San Diego, CA). Default program parameters were used for docking, except that the 'Thoroughness' value was set at 10. This allows the program to undertake a more detailed analysis of the different poses adopted by the compound during the docking procedure. ICM scores obtained from these analyses provided an estimate of the likelihood of small molecule binding. This score (lower is better) is based upon the following parameters: hydrogen bond interactions between the small molecule and the active site; the internal force field energy of the ligand; differences in solvation energies upon ligand binding; loss of entropy from unbound and bound conditions; hydrophobic and electrostatic energies; and H-bond acceptor and donor desolvation. Images of docking poses were then generated by displaying the three catalytic amino acids (S221, E353, H464) and removing the protein ribbon. Distances from the serine Oγ atom to the carbonyl or hydroxyl carbon atoms within the small molecules were determined from the respective docking file.

Small molecule x-ray crystallography

Selected crystals were affixed to MiTeGen sample supports with low-viscosity cryogenic oil, and flash cooled to 100K for x-ray analysis on a Bruker X8 κ diffractometer. The crystal was illuminated with the X-ray beam from a Bruker IμSCu microfocus sealed tube with the resulting images being integrated using SAINT software (Bruker) using a narrow-frame algorithm. A multi-scan absorption correction was applied, and data were corrected for inter-frame

scaling differences with SADABS. The structure was solved via the SHELXTL software package and refined via SHELXL 2014 (Bruker). Hydrogen atoms were placed in idealized positions, and refined according to a riding model. Coordinates for all structures have been deposited at the Cambridge Crystallographic Data Centre (CCDC).

The atom coordinates for compounds **24** and **25**, AMNPQH10 and XANRUB, respectively, were obtained from the Cambridge Structural Database and analyzed using Mercury software.

In vivo inhibition of oseltamivir and irinotecan metabolism

To assess inhibition of oseltamivir, 1 x 10^5 U373MGhCE1 cells were plated into individual wells of a 96 well plated and allowed to attach overnight. The next day, inhibitor (5 μM) was added to cells and after 30 min, the media was removed and replaced with fresh media containing 20 μM oseltamivir and 5 μM inhibitor. After 30 min, the media was removed, an equal volume of acetonitrile was added, and the concentrations of metabolites in these samples were determined by UPLC-MS. Assays for the inhibition of hydrolysis of irinotecan were performed as previously described.[34]

All assays were run in duplicate, and DMSO was used as a control. In addition, blank samples (i.e., media lacking cells) were analyzed and these concentration values were subtracted from all results.

Ancillary Information

Supporting Information. The synthetic methods and physical parameters for previously described compounds; the UPLC traces and ^{1}H, ^{13}C and ^{19}F (as appropriate) spectra for all molecules; the crystallographic data and coordinates for compounds **2**, **9**, **16**, and **23**; and, cell growth inhibition curves for compounds **16**, **18** and **19**.

The CCDC codes for molecules **2**, **9**, **16** and **23** are 1526906, 1526905, 1526907 and 1526904, respectively. Authors will release the atomic coordinates and experimental data upon article publication.

Molecular Formula Strings information for all compounds are also included as Supporting Information.

Corresponding author: Philip M. Potter, Department of Chemical Biology and Therapeutics, St. Jude Children's Research Hospital, 262 Danny Thomas Place, Memphis, TN 38105, United States
Tel: 901-595-6045; Fax: 901-595-4293; E-mail: phil.potter@stjude.org.

Acknowledgements
This work was supported in part by NIH grants CA108775 and AT007531, a Cancer Center Core grant CA21765, and by the American Lebanese Syrian Associated Charities (ALSAC) and St. Jude Children’s Research Hospital

(SJCRH). We thank William Pomerantz for helpful discussions with interpretation of the ^{19}F NMR spectra.

Abbreviations Used: AChE – acetylcholinesterase ; ATCh – acetylthiocholine; CCDC – Cambridge Crystallographic Data Centre; CE – carboxylesterase; irinotecan – 7-ethyl-10-[4-(1-piperidino)-1-piperidino]carbonyloxycamptothecin; hCE1 – human liver CE, CES1; hiCE – human intestinal CE, CES2; IC_{50} – concentration of drug required to inhibit cell growth by 50%; o-NPA – o-nitrophenyl acetate.

REFERENCES

(1) Redinbo, M. R.; Bencharit, S.; Potter, P. M. Human carboxylesterase 1: from drug metabolism to drug discovery. *Biochem. Soc. Trans.* **2003,** *31*, 620-624.

(2) Cashman, J.; Perroti, B.; Berkman, C.; Lin, J. Pharmacokinetics and molecular detoxification. *Environ. Health Perspect.* **1996,** *104*, 23-40.

(3) Hatfield, M. J.; Tsurkan, L.; Hyatt, J. L.; Yu, X.; Edwards, C. C.; Hicks, L. D.; Wadkins, R. M.; Potter, P. M. Biochemical and molecular analysis of carboxylesterase-mediated hydrolysis of cocaine and heroin. *Br. J. Pharmacol.* **2010,** *160*, 1916-1928.

(4) Khanna, R.; Morton, C. L.; Danks, M. K.; Potter, P. M. Proficient metabolism of CPT-11 by a human intestinal carboxylesterase. *Cancer Res.* **2000,** *60*, 4725-4728.

(5) Potter, P. M.; Pawlik, C. A.; Morton, C. L.; Naeve, C. W.; Danks, M. K. Isolation and partial characterization of a cDNA encoding a rabbit liver carboxylesterase that activates the prodrug Irinotecan (CPT-11). *Cancer Res.* **1998,** *52*, 2646-2651.

(6) Tanizawa, A.; Fujimori, A.; Fujimori, Y.; Pommier, Y. Comparison of topoisomerase I inhibition, DNA damage, and cytotoxicity of camptothecin derivatives presently in clinical trials. *J. Natl. Cancer Inst.* **1994,** *86*, 836-842.

(7) Quinney, S. K.; Sanghani, S. P.; Davis, W. I.; Hurley, T. D.; Sun, Z.; Murry, D. J.; Bosron, W. F. Hydrolysis of capecitabine to 5'-deoxy-5-fluorocytidine by human carboxylesterases and inhibition by loperamide. *J. Pharmacol. Exp. Ther.* **2005,** *313*, 1011-1016.

(8) Shi, D.; Yang, J.; Yang, D.; LeCluyse, E. L.; Black, C.; You, L.; Akhlaghi, F.; Yan, B. Anti-influenza prodrug oseltamivir is activated by carboxylesterase human carboxylesterase 1, and the activation is inhibited by antiplatelet agent clopidogrel. *J. Pharmacol. Exp. Ther.* **2006,** *319*, 1477-1484.

(9) Alexson, S. E.; Diczfalusy, M.; Halldin, M.; Swedmark, S. Involvement of liver carboxylesterases in the in vitro metabolism of lidocaine. *Drug Metab. Dispos.* **2002,** *30*, 643-647.

(10) Zhang, J.; Burnell, J. C.; Dumaual, N.; Bosron, W. F. Binding and hydrolysis of meperidine by human liver carboxylesterase hCE-1. *J. Pharmacol. Exp. Ther.* **1999,** *290*, 314-318.

(11) Morton, C. L.; Iacono, L.; Hyatt, J. L.; Taylor, K. R.; Cheshire, P. J.; Houghton, P. J.; Danks, M. K.; Stewart, C. F.; Potter, P. M. Metabolism and antitumor activity of CPT-11 in plasma esterase-deficient mice. *Cancer Chemother. Pharmacol.* **2005,** *56*, 629-636.

(12) Wierdl, M.; Morton, C. L.; Weeks, J. K.; Danks, M. K.; Harris, L. C.; Potter, P. M. Sensitization of human tumor cells to CPT-11 via adenoviral-mediated delivery of a rabbit liver carboxylesterase. *Cancer Res.* **2001,** *61*, 5078-5082.

(13) Wadkins, R. M.; Hyatt, J. L.; Wei, X.; Yoon, K. J.; Wierdl, M.; Edwards, C. C.; Morton, C. L.; Obenauer, J. C.; Damodaran, K.; Beroza, P.; Danks, M. K.; Potter, P. M. Identification and characterization of novel benzil (diphenylethane-1,2-dione) analogues as inhibitors of mammalian carboxylesterases. *J. Med. Chem.* **2005,** *48*, 2905-2915.

(14) Hatfield, M. J.; Tsurkan, L. G.; Hyatt, J. L.; Edwards, C. C.; Lemoff, A.; Jeffries, C.; Yan, B.; Potter, P. M. Modulation of esterified drug metabolism by tanshinones from Salvia miltiorrhiza ("Danshen"). *J. Nat. Prod.* **2013,** *76*, 36-44.

(15) Pardee, A. B.; Li, Y. Z.; Li, C. J. Cancer therapy with beta-lapachone. *Curr. Cancer Drug Targets* **2002,** *2*, 227-242.

(16) Fieser, L. F. 1,2-Naphthoquinone. *Org. Syn.* **1937,** *17*, 68.

(17) Hicks, L. D.; Hyatt, J. L.; Moak, T.; Edwards, C. C.; Tsurkan, L.; Wierdl, M.; Ferreira, A. M.; Wadkins, R. M.; Potter, P. M. Analysis of the inhibition of mammalian carboxylesterases by novel fluorobenzoins and fluorobenzils. *Bioorg. Med. Chem.* **2007,** *15*, 3801-3817.

(18) Hyatt, J. L.; Moak, T.; Hatfield, J. M.; Tsurkan, L.; Edwards, C. C.; Wierdl, M.; Danks, M. K.; Wadkins, R. M.; Potter, P. M. Selective inhibition of carboxylesterases by isatins, indole-2,3-diones. *J. Med. Chem.* **2007,** *50*, 1876-1885.

(19) Hyatt, J. L.; Stacy, V.; Wadkins, R. M.; Yoon, K. J.; Wierdl, M.; Edwards, C. C.; Zeller, M.; Hunter, A. D.; Danks, M. K.; Crundwell, G.; Potter, P. M. Inhibition of carboxylesterases by benzil (diphenylethane-1,2-dione) and heterocyclic analogues is dependent upon the aromaticity of the ring and the flexibility of the dione moiety. *J. Med. Chem.* **2005,** *48*, 5543-5550.

(20) Hyatt, J. L.; Wadkins, R. M.; Tsurkan, L.; Hicks, L. D.; Hatfield, M. J.; Edwards, C. C.; Ii, C. R.; Cantalupo, S. A.; Crundwell, G.; Danks, M. K.; Guy, R. K.; Potter, P. M. Planarity and constraint of the carbonyl groups in 1,2-diones are determinants for selective inhibition of human carboxylesterase 1. *J. Med. Chem.* **2007,** *50*, 5727-5734.

(21) Li, Y.; Li, C. J.; Yu, D.; Pardee, A. B. Potent induction of apoptosis by beta-lapachone in human multiple myeloma cell lines and patient cells. *Mol. Med.* **2000,** *6*, 1008-15.

(22) Di Chenna, P. H.; Benedetti-Doctorovich, V.; Baggio, R. F.; Garland, M. T.; Burton, G. Preparation and cytotoxicity toward cancer cells of mono(arylimino) derivatives of beta-lapachone. *J. Med. Chem.* **2001,** *44*, 2486-2489.

(23) Planchon, S. M.; Pink, J. J.; Tagliarino, C.; Bornmann, W. G.; Varnes, M. E.; Boothman, D. A. beta-Lapachone-induced apoptosis in human prostate cancer cells: involvement of NQO1/xip3. *Exp. Cell Res.* **2001,** *267*, 95-106.

(24) Tseng, C. H.; Cheng, C. M.; Tzeng, C. C.; Peng, S. I.; Yang, C. L.; Chen, Y. L. Synthesis and anti-inflammatory evaluations of beta-lapachone derivatives. *Bioorg. Med. Chem.* **2013,** *21*, 523-531.

(25) Webb, J. L. *Enzyme and Metabolic Inhibitors. Volume 1. General Principles of Inhibition*. Academic Press Inc.: New York, 1963.

(26) Nakamura, Y.; Komatsu, Y.; Hosokawa, Y.; Nakashima, T.; Nakashima, N.; Yano, H.; Hashimoto, T.; Nakashima, H.; Takeya, S. Generalized cytomegalic inclusion disease in neonates and infants. *Acta Pathol. Jpn.* **1980,** *30*, 347-354.

(27) Yano, H.; Yamasaki, M.; Shimomura (nee Sakai), Y.; Iwasaki, M.; Ohta, M.; Furun, Y.; Kouno, K.; Ono, Y.; Ueda, Y. Tautomersim of 4-amino and 4-arylamino-1,2-naphthoquinones. *Chem. Pharm. Bull.* **1980,** *28*, 1207-1213.

(28) Biggs, I. D.; Tedder, J. M. The preparation, spectra and tautomerism of some 4(N-arylamino)-1,2-naphthoquinones. *Tetrahedron* **1978,** *34*, 1377-1380.

(29) Wierdl, M.; Tsurkan, L.; Hyatt, J. L.; Edwards, C. C.; Hatfield, M. J.; Morton, C. L.; Houghton, P. J.; Danks, M. K.; Redinbo, M. R.; Potter, P. M. An

improved human carboxylesterase for enzyme/prodrug therapy with CPT-11. *Cancer Gene Ther.* **2008,** *15*, 183-192.

(30) Hicks, L. D.; Hyatt, J. L.; Stoddard, S.; Tsurkan, L.; Edwards, C. C.; Wadkins, R. M.; Potter, P. M. Improved, selective, human intestinal carboxylesterase inhibitors designed to modulate 7-ethyl-10-[4-(1-piperidino)-1-piperidino]carbonyloxycamptothecin (Irinotecan; CPT-11) toxicity. *J. Med. Chem.* **2009,** *52*, 3742-3752.

(31) Hatfield, M. J.; Tsurkan, L.; Garrett, M.; Shaver, T.; Edwards, C. C.; Hyatt, J. L.; Hicks, L. D.; Potter, P. M. Organ-specific carboxylesterase profiling identifies the small intestine and kidney as major contributors of activation of the anticancer prodrug CPT-11. *Biochem. Pharmacol.* **2011,** *81*, 24-31.

(32) Wadkins, R. M.; Hyatt, J. L.; Yoon, K. J.; Morton, C. L.; Lee, R. E.; Damodaran, K.; Beroza, P.; Danks, M. K.; Potter, P. M. Discovery of novel selective inhibitors of human intestinal carboxylesterase for the amelioration of irinotecan-induced diarrhea: synthesis, quantitative structure-activity relationship analysis, and biological activity. *Mol. Pharmacol.* **2004,** *65*, 1336-1343.

(33) Morton, C. L.; Potter, P. M. Comparison of *Escherichia coli, Saccharomyces cerevisiae, Pichia pastoris, Spodoptera frugiperda* and COS7 cells for recombinant gene expression: Application to a rabbit liver carboxylesterase. *Mol. Biotechnol.* **2000,** *16*, 193-202.

(34) Hyatt, J. L.; Tsurkan, L.; Wierdl, M.; Edwards, C. C.; Danks, M. K.; Potter, P. M. Intracellular inhibition of carboxylesterases by benzil: Modulation of CPT-11 cytotoxicity. *Mol. Cancer Ther.* **2006,** *5*, 2281-2288.

(35) Awad, W. I.; Hafez, M. S. Studies on 4-substituted-β-napthoquinones. *J. Am. Chem. Soc.* **1958,** *80*, 6057-6060.

(36) Gornostaev, L. M.; Lyashchenko, T. A.; Arnold, E. V. The synthesis of benzo[a]phenazine-5,6-dione 7-oxides. *Chem. Het. Compound* **2014,** *49*, 1827-1830.

(37) Singh, P.; Baheti, A.; Thomas, K. R. Synthesis and optical properties of acidochromic amine-substituted benzo[a]phenazines. *J. Org. Chem.* **2011,** *76*, 6134-6145.

(38) Akaike, H. Information Theory and an Extension of the Maximum Likelihood Principle. In *Proceedings of the Second International Symposium on Information Theory*; Petrov, B.N., Csaki, F., Eds.; Akademiai Kiado: Budapest, 1973; pp 267-281.

(39) Akaike, H. A new look at the statistical model identification. *IEEE Trans. Autom. Control* **1974,** *AC-19*, 716-723.

(40) Doctor, B. P.; Toker, L.; Roth, E.; Silman, I. Microtiter assay for acetylcholinesterase. *Anal. Biochem.* **1987,** *166*, 399-403.

Table 1. Esterase inhibition data for **1**, 4-substituted 4-phenoxynaphthalene-1,2-diones (**2**-**8**) and 4-substituted 4-(phenylamino)naphthalene-1,2-diones (**9**-**15**).

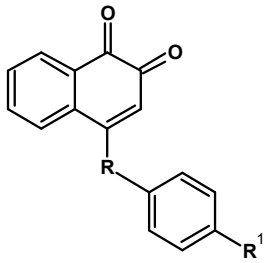

ID	R	R^1	K_i (nM ± SE; o-NPA)		Enzyme inhibition (% at 10μM; o-NPA)		AChE inhibition (% at 10μM; ATCh)
			hCE1	hiCE	hCE1	hiCE	
1	See Fig 1 for structure		1,220 ± 30	109 ± 13	ND[a]	ND	10
2	O	H	23.8 ± 1.9	199.8 ± 18.9	ND	ND	11
3	O	MeO	17.8 ± 1.4	195.5 ± 19.0	ND	ND	18
4	O	Me	4.44 ± 0.5	61.5 ± 1.3	ND	ND	8
5	O	F	45.3 ± 4.5	182.2 ± 20.2	ND	ND	22
6	O	Cl	18.9 ± 2.0	127.4 ± 10.1	ND	ND	31
7	O	Br	14.3 ± 1.4	110.0 ± 9.4	ND	ND	26
8	O	I	4.7 ± 2.5	33.9 ± 2.5	ND	ND	25
9	NH	H	ND	ND	30	12	5
10	NH	MeO	ND	ND	26	12	5
11	NH	Me	ND	ND	44	15	17
12	NH	F	ND	ND	40	14	21
13	NH	Cl	ND	ND	33	22	23
14	NH	Br	ND	ND	26	12	16
15	NH	I	ND	ND	41	10	16

[a] ND – Not determined

Table 2. Esterase inhibition data for 4-substituted (4-phenyl(methyl)amino)naphthalene-1,2-diones (**16**-**22**).

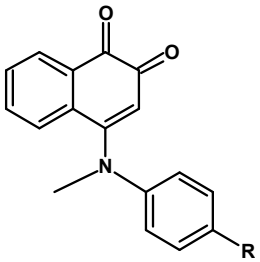

ID	R	hCE1 K_i (nM ± SE; o-NPA)	hCE1 K_i (nM ± SE; oseltamivir)	hiCE inhibition (% at 10μM; o-NPA)	hiCE K_i (nM ± SE; o-NPA)	AChE inhibition (% at 10μM; ATCh)
16	H	90.0 ± 5.2	32.1 ± 4.2	33	ND[a]	3
17	MeO	81.6 ± 4.7	17.7 ± 1.2	7	ND	1
18	Me	11.1 ± 0.2	4.9 ± 0.5	25	ND	3
19	F	163 ± 11	37.6 ± 2.4	19	ND	1
20	Cl	19.2 ± 0.75	12.9 ± 1.3	30	ND	4
21	Br	16.1 ± 0.66	17.2 ± 1.2	52	1,840 ± 105	12
22	I	408 ± 25	148 ± 14	83	284 ± 13	31

[a] ND – Not determined

Figure legends

Figure 1. Structures of the molecules used in the described studies.

Figure 2. Docking of **1**, and selected phenoxy naphthalene-1,2-diones and phenylamino naphthalene-1,2-diones in the active site of hCE1. All compounds were docked using ICMPro software and the X-ray coordinates for hCE1 (RCSB code 1MX1). The catalytic triad of amino acids (S221, H464, E353) that are required for enzyme hydrolysis are indicated in panels a and b. Distances from the serine Oγ atom to the carbonyl carbon atoms in the small molecules are indicated in Ångstroms.

a and b – Two poses of compound **1** (ICM score -19.71); c – compound **2** (ICM score -10.43); d – compound **9** (ICM score -4.40); e – compound **6** (ICM score -11.57); f – compound **13** (ICM score -5.70); g – compound **3** (ICM score -6.49); h – compound **10** (ICM score 0.67).

Figure 3. Docking poses of tautomers of phenoxynaphthalene-1,2-dione and phenyl(methyl)amino naphthalene-1,2-diones in the hCE1 active site. Molecules were docked using ICMPro software and the X-ray coordinates for hCE1 (RCSB code 1MX1).

a - The expected tautomers of compound **9**.

b. Methylation of the N atom in compound **9** to yield **16**, prevents generation of the imino hydroxy derivative.

c. Docking of the imino form of compound **9** into the active site of hCE1 (ICM score -2.92).

d. Docking of compound **16** into the active site of hCE1 (ICM score 5.47).

In panels c and d, the catalytic triad of amino acids is indicated and distances from the serine Oγ atom to the carbonyl or hydroxyl carbon atoms in the small molecules are indicated in Ångstroms.

Figure 4. A schematic indicating the lengths of various bonds determined from the crystal structures of selected naphthalene-1,2-diones.

The shortest bonds are indicated in red font, and the longest in blue. All bond lengths are reported in Ångstroms.

Figure 5. ^{19}F NMR and UV spectra of selected 1,2-dione analogues under different solvent conditions.

a. ^{19}F NMR of **5** in DMSO;

b. ^{19}F NMR of **5** in DMSO containing 5mm TEA;

c. ^{19}F NMR of **12** in DMSO;

d. ^{19}F NMR of **12** in DMSO containing 5mm TEA;

e. ^{19}F NMR of **19** in DMSO;

f. ^{19}F NMR of **19** in DMSO containing 5mm TEA;

g. UV spectra of **2** at pH values ranging from 3-11;

h. UV spectra of **9** at pH values ranging from 3-11;

j. UV spectra of **16** at pH values ranging from 3-11,

In the NMR spectra the signal at ~-113.15ppm results from the standard, fluorobenzene, and in the UV analyses samples were dissolved in 20% DMSO/80% 200mM NaH_2PO_4.

Figure 6. Inhibition of oseltamivir and irinotecan hydrolysis by selected phenoxynaphthalene-1,2-diones and phenyl(methyl)aminonaphthalene-1,2-diones in U373MG cells.

a – Inhibition of hCE1-mediated oseltamivir carboxylate formation by **1** and phenoxynaphthalene-1,2-diones (**2**-**7**).

b – Inhibition of hCE1-mediated oseltamivir carboxylate formation by phenyl(methyl)aminonaphthalene-1,2-diones (**16**-**21**).

c – Inhibition of hiCE-mediated 7-ethyl-10-hydroxycamptothecin formation by **1** and phenoxynaphthalene-1,2-diones (**2**-**7**).

d – Inhibition of hiCE-mediated 7-ethyl-10-hydroxycamptothecin formation by N-methyl naphthalene-1,2-diones (**16**-**21**).

For all plots, C represents control (DMSO) treated samples. Also note the split in the scale on the ordinate axes for panel b. Values above the bars represent the percentage of metabolite formed as compared to DMSO treatment (100%). Statistically significant differences in the results ($p<0.05$), as compared to the control sample, are indicated by an asterisk.

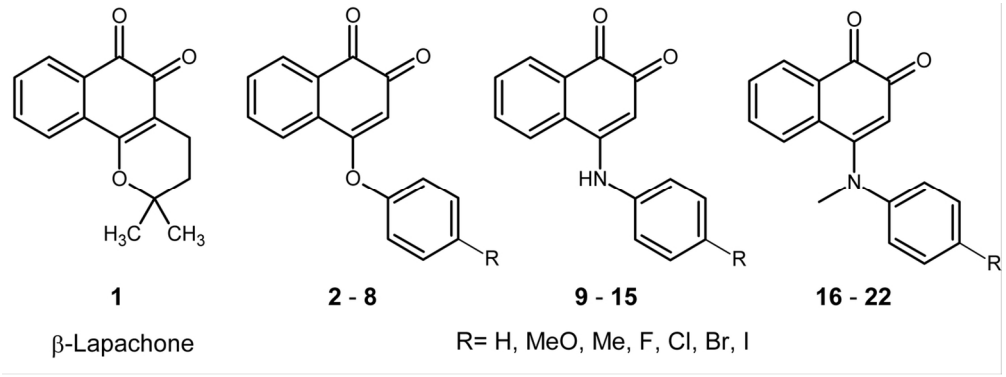

Figure 1. Structures of the molecules used in the described studies.

64x23mm (600 x 600 DPI)

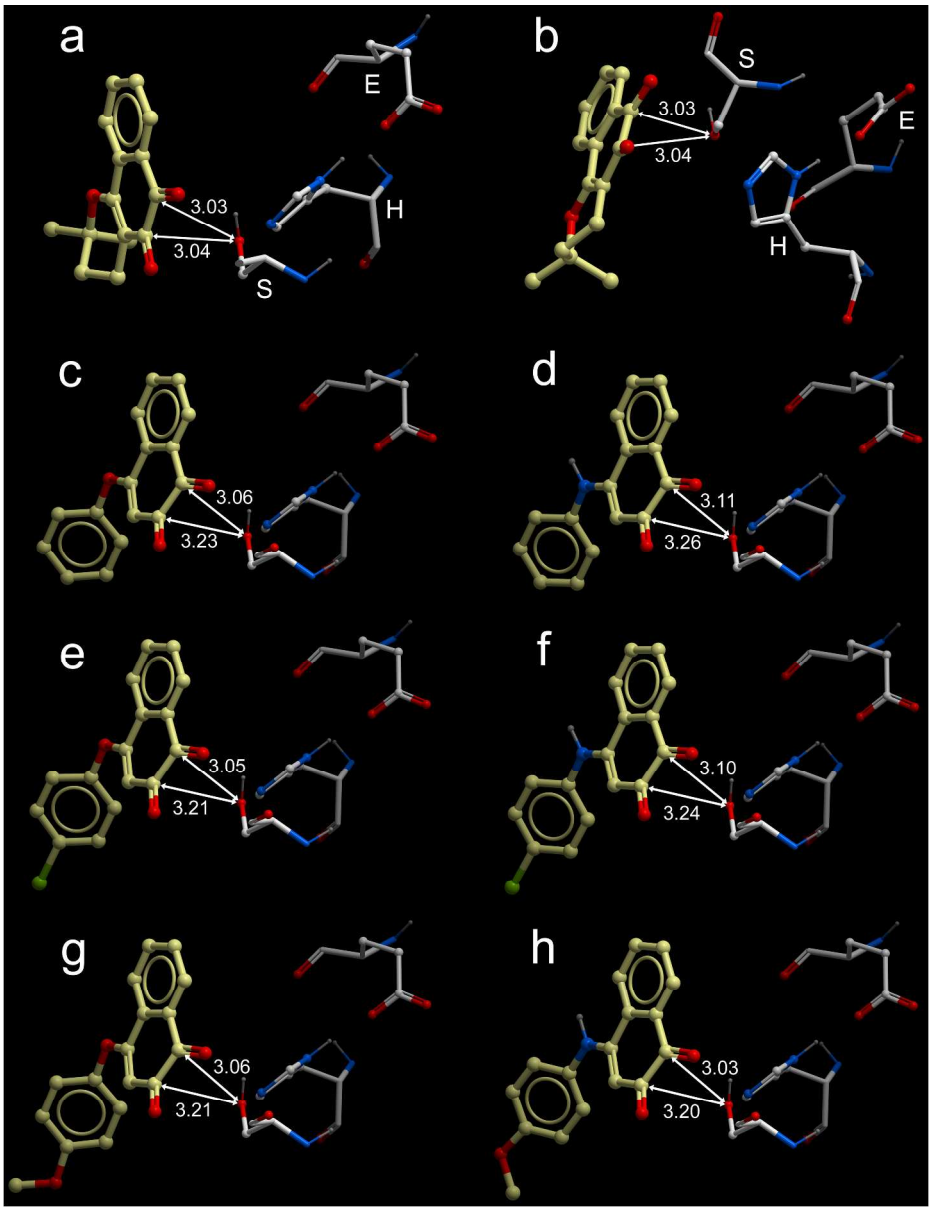

Figure 2. Docking of **1**, and selected phenoxy naphthalene-1,2-diones and phenylamino naphthalene-1,2-diones in the active site of hCE1. All compounds were docked using ICMPro software and the X-ray coordinates for hCE1 (RCSB code 1MX1). The catalytic triad of amino acids (S221, H464, E353) that are required for enzyme hydrolysis are indicated in panels a and b. Distances from the serine Oγ atom to the carbonyl carbon atoms in the small molecules are indicated in Ångstroms.┬ a and b – Two poses of compound **1** (ICM score -19.71); c – compound **2** (ICM score -10.43); d – compound **9** (ICM score -4.40); e – compound **6** (ICM score -11.57); f – compound **13** (ICM score -5.70); g – compound **3** (ICM score -6.49); h – compound **10** (ICM score 0.67).┬

264x343mm (300 x 300 DPI)

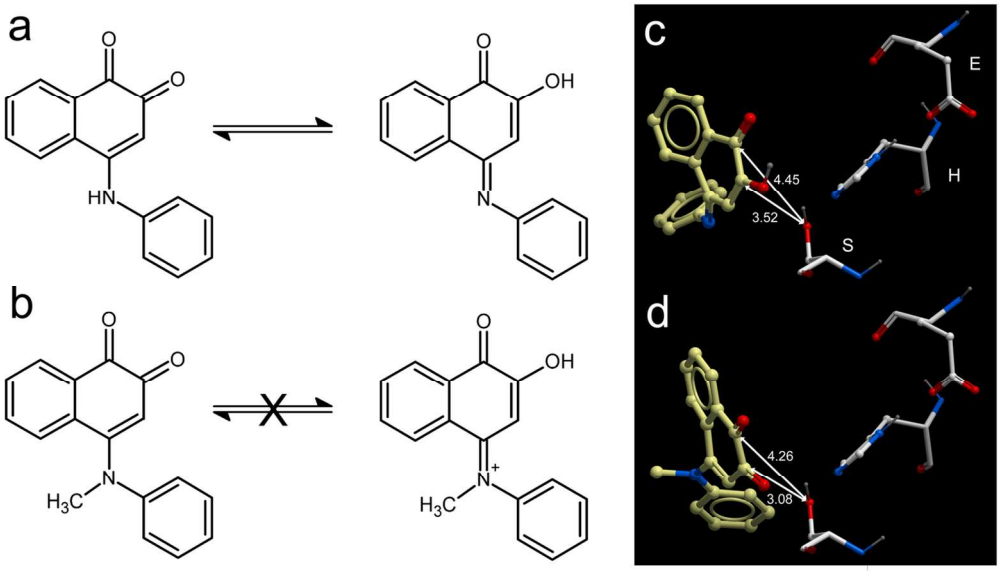

Figure 3. Docking poses of tautomers of phenoxynaphthalene-1,2-dione and phenyl(methyl)amino naphthalene-1,2-diones in the hCE1 active site. Molecules were docked using ICMPro software and the X-ray coordinates for hCE1 (RCSB code 1MX1). a - The expected tautomers of compound **9**. b. Methylation of the N atom in compound **9** to yield **16**, prevents generation of the imino hydroxy derivative. c. Docking of the imino form of compound **9** into the active site of hCE1 (ICM score -2.92). d. Docking of compound **16** into the active site of hCE1 (ICM score 5.47). In panels c and d, the catalytic triad of amino acids is indicated and distances from the serine Oγ atom to the carbonyl or hydroxyl carbon atoms in the small molecules are indicated in Ångstroms.

63x35mm (600 x 600 DPI)

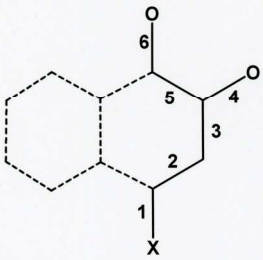

Bond 1 – **24** < **9** < **2** < **16** < **25**
Bond 2 – **2** = **23** < **25** < **16** < **9** < **24**
Bond 3 – **24** < **9** < **16** < **2** = **25** < **23**
Bond 4 – **25** < **2** = **23** < **16** < **9** < **24**
Bond 5 – **24** < **25** < **2** = **19** = **16** < **23**
Bond 6 – **24** = **9** < **2** = **16** = **23** = **25**

Compound	Bond length (Å)						Likelihood of imine formation
	1	2	3	4	5	6	
2 (X=OPh)[a]	1.360	1.342	1.445	1.218	1.540	1.216	N/A
9 (X=NPh)[a]	1.352	1.380	1.412	1.247	1.540	1.210	High
16 (X=N(Me)Ph)[a]	1.374	1.371	1.429	1.232	1.537	1.217	Low
1,2-Naphthoquinone (**23**; X=H)[a]	(0.95)[b]	1.346	1.452	1.218	1.552	1.217	N/A
4-Amino-1,2-naphthoquinone[c] (**24**; X=NH_2)	1.322	1.407	1.381	1.263	1.504	1.208	High
4-(9H-Carbazol-9-yl)-1,2-naphthoquinone[d] (**25**; X=NR_1R_2 - pyrrole ring of carbazole moeity)	1.411	1.352	1.448	1.205	1.530	1.218	Low

[a] – Detailed structural parameters are included in the Supporting Information
[b] – Bond 1 in compound **23** is C-H
[c] – Data taken from CSD – Accession code AMNPQH10
[d] – Data taken from CSD – Accession code XANRUB

Figure 4. A schematic indicating the lengths of various bonds determined from the crystal structures of selected naphthalene-1,2-diones.
The shortest bonds are indicated in red font, and the longest in blue. All bond lengths are reported in Ångstroms.

157x134mm (300 x 300 DPI)

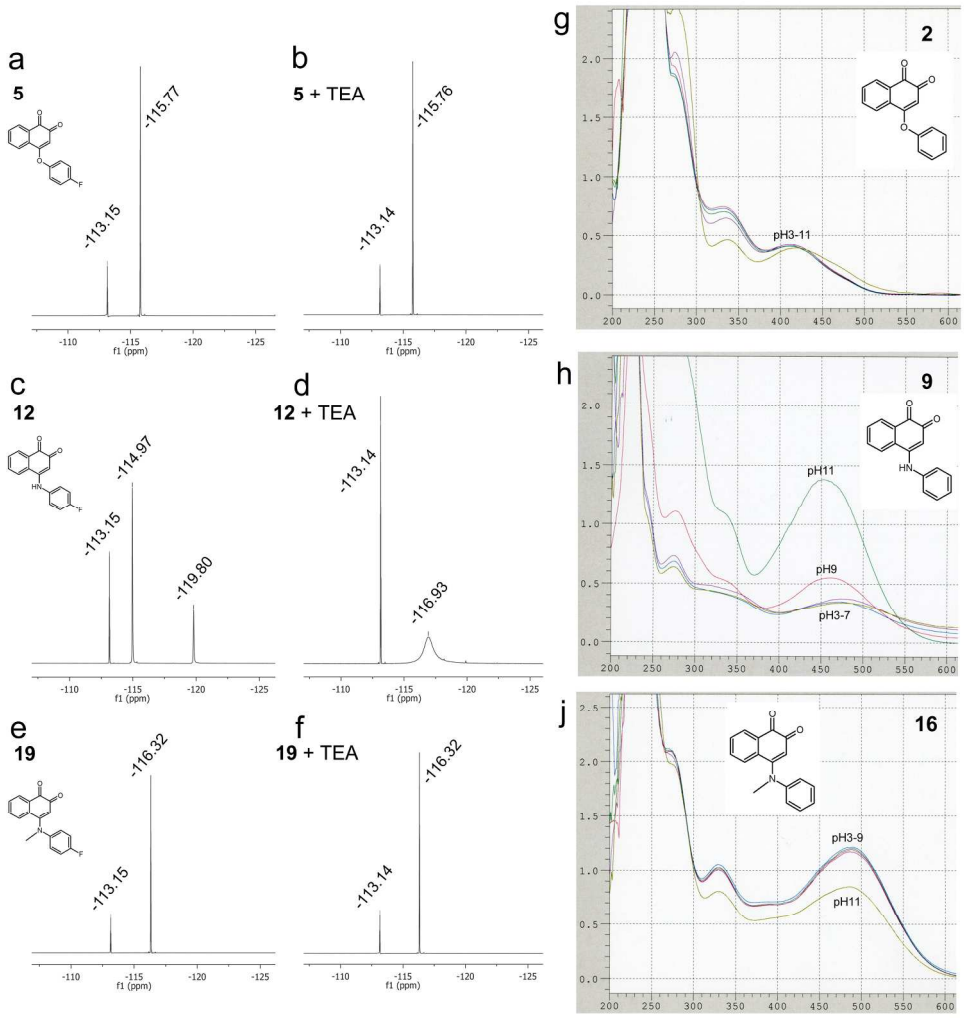

Figure 5. ^{19}F NMR and UV spectra of selected 1,2-dione analogues under different solvent conditions. ┬ a. ^{19}F NMR of **5** in DMSO;┬ b. ^{19}F NMR of **5** in DMSO containing 5mm TEA;┬ c. ^{19}F NMR of **12** in DMSO;┬ d. ^{19}F NMR of **12** in DMSO containing 5mm TEA;┬ e. ^{19}F NMR of **19** in DMSO; ┬ f. ^{19}F NMR of **19** in DMSO containing 5mm TEA;┬ g. UV spectra of **2** at pH values ranging from 3-11;┬ h. UV spectra of **9** at pH values ranging from 3-11;┬ j. UV spectra of **16** at pH values ranging from 3-11,┬ In the NMR spectra the signal at ~-113.15ppm results from the standard, fluorobenzene, and in the UV analyses samples were dissolved in 20% DMSO/80% 200mM NaH_2PO_4.┬

228x233mm (300 x 300 DPI)

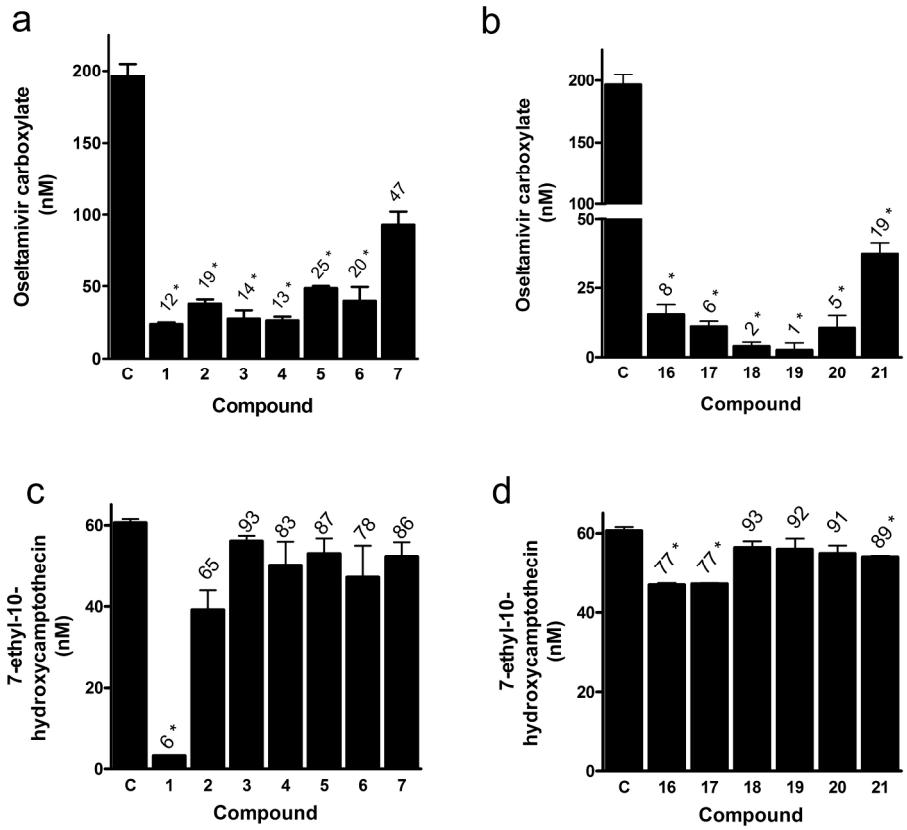

Figure 6. Inhibition of oseltamivir and irinotecan hydrolysis by selected phenoxynaphthalene-1,2-diones and phenyl(methyl)aminonaphthalene-1,2-diones in U373MG cells.┼ a – Inhibition of hCE1-mediated oseltamivir carboxylate formation by **1** and phenoxynaphthalene-1,2-diones (**2**-**7**).┼ b – Inhibition of hCE1-mediated oseltamivir carboxylate formation by phenyl(methyl)aminonaphthalene-1,2-diones (**16**-**21**).┼ c – Inhibition of hiCE-mediated 7-ethyl-10-hydroxycamptothecin formation by **1** and phenoxynaphthalene-1,2-diones (**2**-**7**).┼ d – Inhibition of hiCE-mediated 7-ethyl-10-hydroxycamptothecin formation by N-methyl naphthalene-1,2-diones (**16**-**21**).┼ For all plots, C represents control (DMSO) treated samples. Also note the split in the scale on the ordinate axes for panel b. Values above the bars represent the percentage of metabolite formed as compared to DMSO treatment (100%). Statistically significant differences in the results ($p<0.05$), as compared to the control sample, are indicated by an asterisk. ┼

245x216mm (300 x 300 DPI)

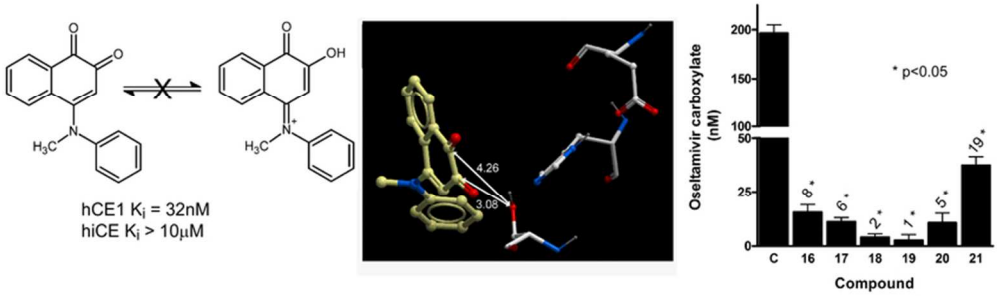

Table of Contents graphic

35x10mm (600 x 600 DPI)